Geophys. J. Int. (2006) **167,** 761–778 doi: 10.1111/j.1365-246X.2006.03127.x

Relocation and assessment of seismicity in the Iran region

E. Robert Engdahl,[1] James A. Jackson,[3] Stephen C. Myers,[2] Eric A. Bergman[1] and Keith Priestley[3]

[1] *Center for Imaging the Earth's Interior, Department of Physics, University of Colorado* 80309-0390, *USA. E-mail: engdahl@colorado.edu*
[2] *Lawrence Livermore National Laboratory, Box* 808 L-205, *Livermore,* CA 94551, *USA*
[3] *Bullard Laboratories, Madingley Rise, Madingley Road, Cambridge,* CB3 0EZ, *UK*

Accepted 2006 July 4. Received 2006 July 3; in original form 2006 April 4

SUMMARY

More than 2000 instrumentally recorded earthquakes occurring in the Iran region during the period 1918–2004 have been relocated and reassessed, with special attention to focal depth, using an advanced technique for 1-D earthquake location. A careful review of starting depths, association of teleseismic depth phases, and the effects of reading errors on these phases are made and, when necessary, waveforms have been examined to better constrain EHB focal depths. Uncertainties in EHB epicentres are on the order of 10–15 km in the Iran region, owing to the Earth's lateral heterogeneity and uneven station distribution. Uncertainties of reviewed EHB focal depth estimates are on the order of 10 km, as compared to about 4 km for long-period *P* and *SH* body-waveform inversions. Nevertheless, these EHB depth estimates are sufficiently accurate to resolve robust differences in focal depth distribution throughout the Iran region and, within their errors, show patterns that are in agreement with the smaller number of earthquakes whose depths have been confirmed by body-wave modelling or local seismic networks. The importance of this result is that future earthquakes with apparently anomalous depths can easily be identified, and checked, if necessary. Most earthquakes in the Iranian continental lithosphere occur in the upper crust, with the crustal shortening produced by continental collision accommodated entirely by thickening and distributed deformation. In the Zagros Mountains nearly all earthquakes are confined to the upper crust (depths <20 km), and there is no evidence for a seismically active subducted slab dipping NE beneath central Iran. By contrast, in southeastern Iran, where the Arabian seafloor is being subducted beneath the Makran coast, low-level earthquake activity occurs in the upper crust as well as to depths of at least 150 km within a northward-dipping subducting slab. Near the Oman Line, a region transitional between the Zagros and the Makran, seismicity extends to depths of up to 30–45 km in the crust, consistent with low-angle thrusting of Arabian basement beneath central Iran. In north-central Iran, along the Alborz mountain belt, seismic activity occurs primarily in the upper crust but with some infrequent events in the lower crust, particularly in the western part of the belt (the Talesh), where the South Caspian basin underthrusts NW Iran. Earthquakes that occur in a band across the central Caspian, following the Apscheron–Balkhan sill between Azerbaijan and Turkmenistan, have depths in the range 30–100 km, deepening northwards. These are thought to be connected with either incipient or remnant northeast subduction of the South Caspian basin basement beneath the east-west trending Apscheron–Balkhan sill. Curiously, in this region of genuine mantle seismicity, there is no evidence for earthquakes shallower than 30 km.

Key words: focal depth, Iran, relocation, seismicity, seismotectonics.

INTRODUCTION

Iran is one of the most seismically active areas in the world. This activity primarily results from its position as a 1000-km-wide zone of compression between the colliding Eurasian and Arabian continents (Fig. 1). However, a comprehensive re-analysis of the reported instrumental seismicity data for Iran has not been published to date. Most detailed studies of earthquakes and their distribution in the Iran region have been conducted in geographically limited areas, often based on global catalogues such as those produced by the

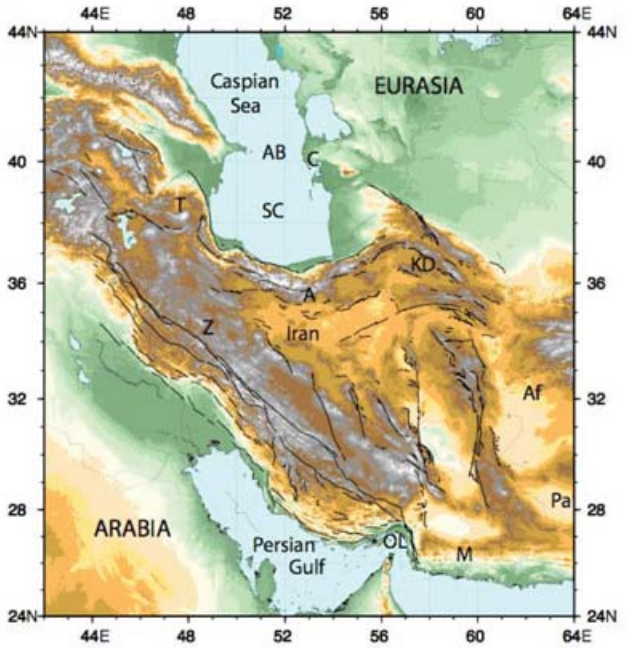

Figure 1. Topographic and active fault map of Iran and surrounding regions. Geographic and tectonic features indicated are: Afghanistan (Af); Pakistan (Pa); Apscheron–Balkhan sill (AB); Cheleken (C); South Caspian basin (SC); Talesh mountains (T); Alborz mountains (A); Kopeh Dagh (KD); Zagros mountains (Z); Oman Line (OL) and and Makran (M). The compilation of faults is courtesy of Richard Walker.

International Seismological Centre (ISC) and the US Geological Survey's National Earthquake Information Center (USGS/NEIC). Depths for many events in these global catalogues, which until only recently were based entirely on first-arrival times of *P* waves, are often not determined with sufficient accuracy for many geological and tectonic purposes. Thus some early researchers (e.g. Nowroozi 1971; Bird *et al.* 1975) suggested that subduction of the continental Arabian shield occurred beneath Iran in the Zagros, based on reported catalogue depths greater than 50 km. However, local seismograph networks have found no reliable depths in the Zagros deeper than ∼20 km, even in places where deeper earthquakes were reported to have occurred (e.g. Niazi *et al.* 1978; Tatar *et al.* 2004). Maggi *et al.* (2000a) and Talebian & Jackson (2004) addressed the depth problem in the Zagros by analysing *P* and *SH* body waveforms of the larger earthquakes there, and again found no evidence for seismicity deeper than 20 km within the main part of the belt. This example from the Zagros serves to illustrate the need to carefully reassess the reliability of catalogue-based depths before using them for geological, tectonic or even seismic-hazard purposes. Since earthquake focal depth distributions are particularly informative features of actively deforming areas, and since those distributions are known to vary geographically within Iran, a principal aim of this study is to provide a uniform assessment of those distributions throughout the whole country, using all available data sources.

In recent years techniques developed by Engdahl *et al.* (1998; EHB) and Engdahl & Villasenor (2002) have resulted in a general improvement in the locations and focal depths of earthquakes globally, including Iran. In this study, we extend the work of Maggi *et al.* (2000a) and Maggi *et al.* (2002) by applying the EHB algorithm, with special attention to focal depth, to all teleseismically detected earthquakes for which the number and distribution of teleseismic recording stations lead us to expect, in principle, a well-constrained location. We extend the time period of our study back beyond the catalogues of the USGS and ISC to the period before 1964, where possible, and continue it through 2004. The earliest earthquakes we consider in the Iran region are from 1918. Ambraseys (1978) and Berberian (1979) compared International Seismological Summary (ISS) locations with well-determined macroseismic areas of moderate-sized earthquakes (with restricted damage zones) to estimate the errors in some of the early instrumental locations, showing that some of them were as large as 100 km. Our relocations for 76 of these historical events result in median location differences of ±24 km from the ISS locations, with some of the earliest events having differences in location of more than 100 km.

The aim of this study is to produce a comprehensive catalogue of all instrumentally recorded events for the region, and to summarize the patterns we see in this relocated seismicity, in particular the patterns of reliable focal depth distributions, within their active tectonic context. Over 2000 instrumentally recorded earthquakes occurring in the Iran region during the period 1918–2004 that are well-constrained by teleseismic arrival times reported to the ISS, ISC and NEIC have been relocated as single events with special attention to focal depth using the EHB methodology (Engdahl *et al.* 1998). The purpose of this study is to expand geographically the work of Maggi *et al.* (2000a). Because they used long-period body waves, Maggi *et al*'s study was limited to earthquakes larger than about M_w 5.4. Our present study looks at very many more earthquakes, including many that are too small for long-period body-wave analysis. We rely on a careful review of EHB starting depths, the EHB assignment of teleseismic depth phases, and the effects of reading errors on these phases. The reviewed EHB depth estimates are sufficiently accurate to resolve robust differences in focal depth distribution within the crust and upper mantle throughout the Iran region, and show patterns in agreement with the more accurate, though numerically far fewer, long-period body-wave inversion depths. A principal result of our study is that the patterns of depth distributions revealed by the relatively small number of earthquakes (∼167) whose depths (±4 km) are confirmed by waveform modelling are now in agreement with the much larger number (∼1229) whose EHB depths (±10 km) have been reassessed, within their respective errors. This is a significant advance, as outliers and future events with apparently anomalous depths can be readily identified and, if necessary, further investigated. A secondary goal is to set a standard for future teleseismic relocation studies of seismicity, in particular focal depth, in other seismically active regions.

METHODS

Early teleseismic location work relied almost exclusively on the use of first-arrival times of *P* phases (Bolt 1960; Engdahl & Gunst 1966). Standard modern teleseismic catalogues produced by the ISC and the USGS/NEIC have also, until only, recently relied almost entirely on first-arrival times of *P* phases, locating events using the Jeffreys-Bullen (JB) traveltime tables (Jeffreys & Bullen 1940). Engdahl *et al.* (1998) have shown that hypocentre determination can be significantly improved by using, in addition to direct *P* and *S* phases, the arrival times of *PKiKP*, *PKPdf* , and the teleseismic depth phases (*pP*, *pwP* and *sP*) in the relocation procedure. Epicentre constraints are improved by the inclusion of *S*-wave and *P*-core phases because their traveltime derivatives differ significantly in magnitude from direct *P*, while depth-origin time trade-off is ameliorated by the inclusion of depth phases (*pP*, *pwP*, *sP*) because their traveltime derivatives are opposite in sign to those of direct *P*.

A problem with the use of later phases is that their correct identification often requires a prior knowledge of the event depth and distance. Recognizing this problem, Kennett *et al.* (1995) and Engdahl *et al.* (1998) included a phase re-association step in their location procedure. In their approach, phase arrivals are re-identified after each iteration using a statistically based association algorithm. Probability density functions (PDFs) for relevant phases, centred on their theoretical relative traveltimes for a given hypocentre, are compared to the observed phase arrivals. When PDFs overlap for a particular phase, the phase identification is assigned in a probabilistic manner (i.e. 'rolling the dice') based on the relevant PDF values, making sure not to assign the same phase to two different arrivals. This procedure is applied for depth phase identification in this study. Nevertheless, a careful review of the automatic depth phase associations for individual events is still necessary to ensure depth uncertainty on the order of 10 km.

The procedures introduced by Engdahl *et al.* (1998) (hereafter referred to as the EHB algorithm), besides including *P*, *S*, and other later-arriving phases in event location, also uses an improved earth model. The earth model used is ak135 (Kennett *et al.* 1995), a derivative of the iasp91 model (Kennett & Engdahl 1991). The most significant differences between the traveltimes predicted by these models and the older JB tables are for upper mantle and core phases. The ak135 model also more accurately predicts the observed traveltimes of later-arriving phases, and is in better agreement with *S*-wave data than the JB tables. The EHB algorithm applies ellipticity corrections based on the ak135 model (Kennett & Gudmundsson 1996), empirical teleseismic station patch corrections (for 5×5 degree patches), and weighting by phase variance as a function of distance (Engdahl 2006). Outliers are removed dynamically by truncating the residual distribution at two standard deviations: approximately 7.5 s for arrivals at epicentral distances up to 28° (surface-focus distance) and 3.5 s at larger (teleseismic) distances.

It is important to point out that the EHB procedure cannot entirely remove the effects of the Earth's lateral heterogeneity on teleseismic earthquake location. van der Hilst & Engdahl (1992) and Bijwaard *et al.* (1998) have shown that in or near subducted lithosphere, where aspherical variations in seismic wave velocities are large (i.e. on the order of 5–10 per cent,) the lateral variations in seismic velocity, the uneven spatial distribution of seismograph stations, and the specific choice of seismic data used to determine the earthquake hypocentre can easily combine to produce bias in teleseismic earthquake epicentres of up to several tens of kilometres. Bondár *et al.* (2003) found that catalogue location accuracy is most reliably estimated by station geometry. In particular, using a large data set of exceptionally well-located earthquakes and nuclear explosions, they found that when station-coverage meets the criterion of a secondary azimuth gap (the largest azimuth gap filled by a single station) of less than 120 degrees, regional and teleseismic networks provide epicentral accuracy of 25 km at the 90 per cent confidence level. In this study we select only events that have ten or more teleseismic observations and a teleseismic secondary azimuth gap <180 degrees.

The EHB method has already been successfully applied to earthquakes reported by the ISC and NEIC during the modern period (1964–2004), providing a uniform database of well-constrained, significantly improved, hypocentres. In addition, the application of this method to historical earthquakes listed in the bulletin of the ISS has resulted in a comprehensive and internally consistent (i.e. same model and location procedures) digital earthquake catalogue for the entire 20th century (Engdahl & Villasenor 2002). In this study nearly all instrumentally recorded events in Iran prior to 1964 have been relocated to provide a catalogue complete above Ms 6.5. Engdahl & Villasenor (2002) note that the central distribution of residuals for pre-1964 earthquakes is only slight larger than earthquakes located from 1964 on, albeit the tails of the distribution are much longer (i.e. there are many more and larger outliers in the older data). Hence, these older events are formally located almost as well as those occurring during the modern period with some events during the 1960s even having sufficient depth constraints to be included in our analyses of depth distribution. For the modern period, our selection criteria provide a catalogue that is complete down to at least M_w 5.5, but includes many events of smaller magnitude.

EHB EPICENTRE ESTIMATES

Kennett & Engdahl (1991) assessed global epicentral location accuracy for a data set of 104 test events (21 nuclear explosions and 83 well-located earthquakes) in the course of developing the IASP91 velocity model and found an average epicentral location error (using IASP91) of 14 km. Engdahl *et al.* (1998) assessed the location accuracy of EHB procedures by relocating a data set of 1166 nuclear explosions plus the 83 earthquakes used as test events by Kennett & Engdahl (1991) and estimated an average epicentral mislocation vector of 9.4 ± 5.7 km. All of the test events had a secondary azimuthal gap of less than 180 degrees. Myers & Schultz (2000) re-examined the EHB data set (excluding subduction zone events) and reached a similar conclusion, estimating 15 km (or better) epicentre accuracy at the 95 per cent confidence level for events with a secondary azimuthal gap of less than 90 degrees.

Engdahl & Bergman (2001) determined highly accurate relative locations for a number of teleseismically well-recorded earthquake clusters in Iran using a multiple event location method. When well-determined local-network (calibration) locations for a subset of events in the clusters are reconciled with the corresponding teleseismic relative locations, the absolute epicentre accuracy for many events in these clusters can be determined to 5 km or better. The reconciliation (or calibration) process determines the shift in the four hypocentral coordinates of the teleseismically determined cluster, maintaining the relative locations, that achieves the best fit with the local-network solutions, taking into account the uncertainty of the local network locations, the uncertainties of the relative locations determined with teleseismic data, and the level of inconsistency if there is more than one calibration event. This single optimal shift is applied to every event in the cluster to provide a bias-free, absolute location with corresponding uncertainty. EHB epicentres for 80 earthquakes in Iran were compared to a set of these highly accurate absolute epicentres determined by Engdahl and Bergman during the post-1964 time period. The average and median mislocation errors were 9.2 ± 5.2 km and 8.9 ± 4.9 km, respectively. The direction of EHB mislocation (or vector bias), though consistent for events in individual clusters, was variable across Iran. This can be accounted for by lateral variations in Earth structure and station coverage between individual clusters. We conclude that the EHB teleseismic epicentre bias for earthquakes in Iran is on the order of $\sim$10 km, at least for the period post-1964 period. Hence, in this period EHB teleseismic epicentre bias in Iran is significantly reduced (but not eliminated) when the teleseismic station coverage is good (teleseismic secondary azimuth gap <180 degrees).

EHB DEPTH ESTIMATES

The use of later arriving phases in routine hypocentre determination potentially provides powerful constraints on focal depth and

reduces the effects of strong near-source lateral velocity heterogeneities. However, both ISC and NEIC have relied, until only recently, almost entirely on first-arrival times of *P* waves to locate earthquakes. Moreover, the reporting of depth phases by ISS was sporadic and for many events the phases were often misidentified. The EHB phase identification algorithm applied to the phase group immediately following the *P* wave at teleseismic distances (*pP*, *pwP*, *sP* and PcP) has been shown to be particularly effective in identifying these phases so that they can be exploited in the relocation procedure. In the following sections we review comparisons of EHB free-depth determinations using the arrival times of associated depth phases with depths determined by other independent methods.

Comparison between EHB and ISC hypocentres

The difference between EHB and ISC epicentres (1964–2002) for teleseismically well-constrained events in our database is not large (median difference of 5.0 km). Engdahl *et al.* (1998) have shown that only a small improvement in location is realized by using a modern earth model (although ak135 does provide a dramatic improvement over JB in later phase identification). For depth estimation, the ISC relies almost entirely on the first-arrival times of *P* waves. However, unless the station distance is within the inflection point of the traveltime curve for an event, where the travel derivative with respect to depth is reversed in sign, these data alone provide only minimal depth resolution. Moreover, the effects of lateral heterogeneity and station coverage for earthquakes in the Iran region usually results in ISC depths that are significantly overestimated as shown in Fig. 2 (median 16.9 km). The lower slanted line in Fig. 2 results from events that the ISC has set at a 33 km default depth. The vertical lines are EHB depths that, after review, have been set at the nearest 5 km depth to obtain a best fit to associated depth-phase arrival times. Deeper events are not as poorly estimated as crustal events by the ISC, possibly because some of those depths have been set based on reported *pP*-*P* differential times. Moreover, for deeper events, the clear time separation between *pP*, *sP* and *P* makes it more likely they will be correctly identified.

Comparison of EHB depths with USGS/NEIC depths determined from broad-band waveforms

Since 1985 October, the USGS/NEIC has been routinely determining a broad-band depth; either from inversion of differential times of depth phases identified on broad-band waveforms (Harvey and Choy, 1982) or by modelling of P and transversely polarized *S* waves with methods described by Choy & Dewey (1988), for most earthquakes of magnitude greater than about M_w 5.5. The waveforms are processed to have a flat response in displacement or velocity over the frequency range 0.01–5.0 Hz, which encompasses spectral information above, about and below the corner frequency of teleseismically recorded earthquakes. The advantage of using broad-band records is that the source-time function (albeit convolved with attenuation) can be viewed, thereby minimizing the trade-off between source function and depth. In contrast, it is less easy to see the separation between the direct and reflected phases in instrument-filtered waveforms, even if that duration is longer than the duration of the source-time function. Fig. 3 compares EHB free-depth solutions using clearly identifiable depth phases with NEIC broad-band depth determinations for 29 events. The observed depth differences are mostly less than 10 km. However, EHB depths appear to be slightly deeper (with a median of 2.2 km).

Comparison of EHB depths with depths determined by long-period *P* and *SH* body-wave modelling

Waveform depths determined by long-period body-wave modelling of the early part of *P* and *SH* waveforms by the Cambridge research group (e.g. Priestley *et al.* 1994; Maggi *et al.* 2000a; Jackson *et al.* 2002; Talebian & Jackson 2004) were a valuable resource for this

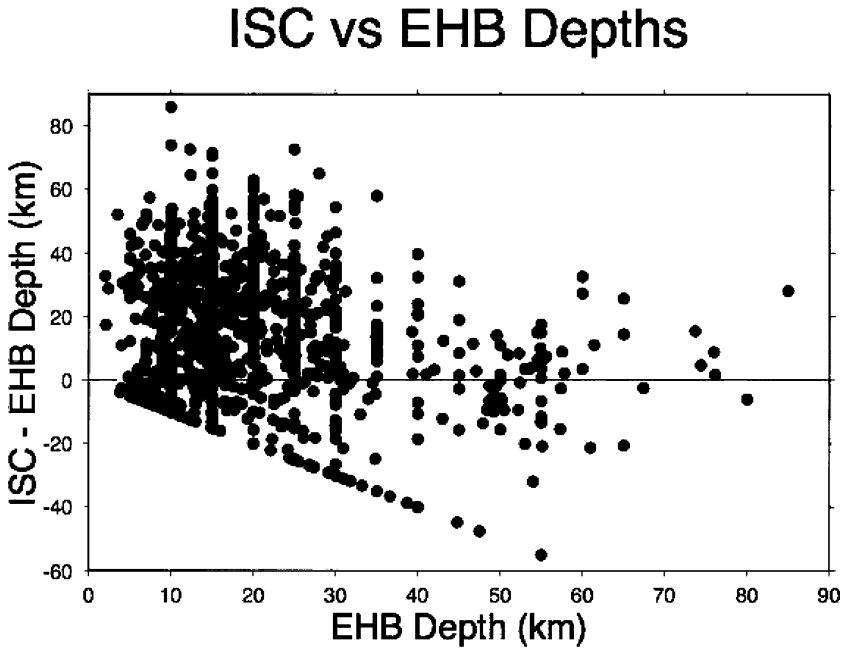

Figure 2. Comparison of EHB reviewed depth estimates based on clearly identifiable depth phases with depths reported by the ISC based only on first-arrival times of *P* phases.

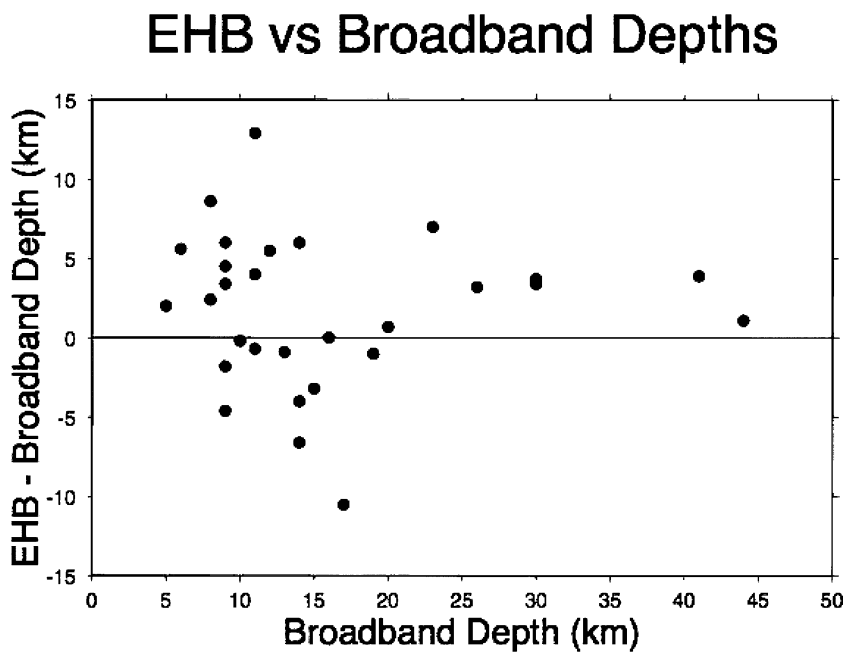

Figure 3. Comparison of EHB free-depth solutions using clearly identifiable depth phases with broad-band depths reported by the USGS/NEIC (1984–2003).

project. The seismograms used for this modelling are narrower in bandwidth than the broad-band records used by the USGS/NEIC, but contain higher frequencies than those used in the routine Harvard CMT determinations (discussed later), and are sensitive to depth for shallow earthquakes. The method looks at the *P*, *pP* and *sP* arrivals in the *P* waveforms and the *S* and *sS* arrivals in the *SH* waveforms. However, for upper-crustal events *pP* and *sP* are usually not visually identifiable as separate from the direct *P* (nor is *sS* separable from direct *S*), so the depths are constrained by modelling the waveforms themselves. This technique can only be applied to earthquakes that generate the relatively long periods used, which are generally about M_w 5.4 or bigger.

The EHB procedure was used to determine unconstrained depth solutions of 151 events that were modelled using long-period *P* and *SH* waveforms for the time period post-1962. Each event had more than five phases that could be identified as *pP* or *sP* depth phases. Starting depths were set at the waveform depths, which have an estimated accuracy of ∼4 km in the Iran region, to avoid secondary minima in the depth determination. Differences between the Cambridge and EHB results are compared as functions of depth and magnitude in Fig. 4. The EHB depths for most events were within 10 km of the corresponding waveform depths, with a maximum difference no larger than 15 km (Fig. 4a). There does not appear to be any magnitude dependence (Fig. 4b). EHB depths are slightly deeper than waveform depth estimates (median 3.1 km) most likely because different reference velocity models were used (ak135 versus source-velocity models that varied regionally for the waveform modelling). The waveform inversion method returns a centroid depth, whereas EHB depths correspond to, in principle, the point of rupture onset or nucleation. They needn't be the same, but for most of the events in this study, which are small, the source dimensions are small enough for them to be quite similar. The systematic difference in depth between waveform depths and EHB depths might, therefore, also be explained if rupture typically initiates near the bottom of the ultimate rupture area.

The outliers for the shallow events shown in Fig. 4 warrant special comment. An outstanding problem is that for some of these relatively large, shallow-focus, complex earthquakes, *pP* often arrives within the source-time function of *P*, which may consist of one or more sub-events. The gross features of the source-time functions of *P* and *pP*, however, may sometimes remain discernible in broad-band displacement records and the exact onset times of depth phases can be further refined by examination of velocity seismograms which are sensitive to small changes in displacement (Choy & Engdahl 1987). In this study, however, we have relied primarily on reported data, usually read from short-period seismograms. When only catalogue-derived short-period depth phases are available, EHB phase identifications often become inconsistent and can result in inappropriate depth estimates (e.g. the larger positive outliers for very shallow depth events in Fig. 4a).

Long-period *P* and *SH* body-wave modelling also has potential problems with large, shallow earthquakes because their complexity commonly offers various opportunities to trade-off depth against time-function duration. Another potential, but minor, problem is the effect of varying regional crustal velocity structure in the source region, which the procedures used by the Cambridge group attempt to allow for, but is not accounted for by the EHB procedure, which uses a standard global reference model (ak135). For example, EHB depth estimates for the two deepest events shown in Fig. 4a, both in the offshore Caspian Sea region, are about 5 km deeper than the depths obtained by long-period body-wave modelling that allows for a 20 km thick overlying low-velocity sediment layer. Hence, at least in this region, the global reference model will translate depth-phase arrival times into deeper focal depths because the assumed crustal velocities are too high.

In summary, for the reasons given above, we believe the accuracy of depths determined by long-period *P* and *SH* body-wave modelling are superior to depths estimated using arrival-time-based EHB procedures and hence adopt them in this study, where they are available.

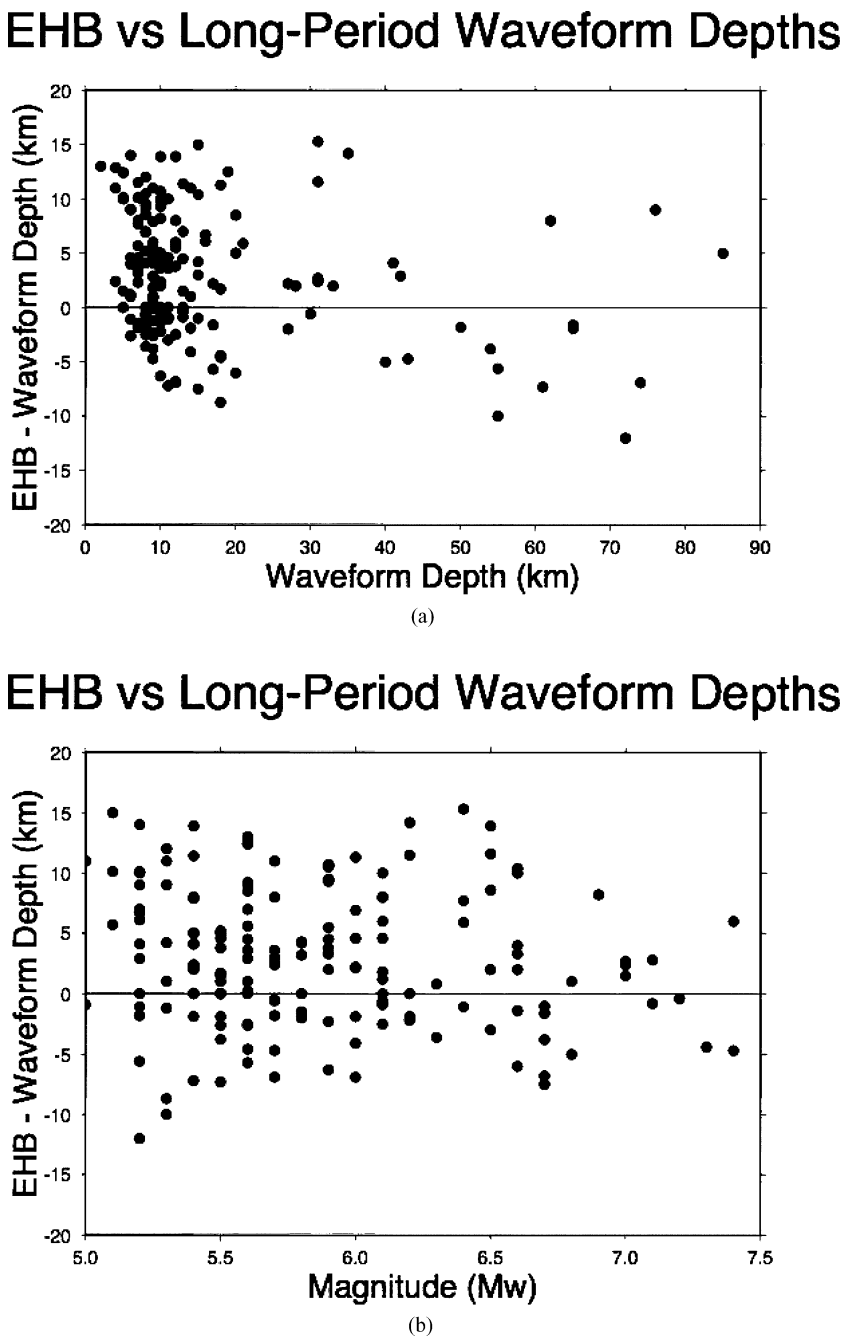

Figure 4. (a) Comparison of EHB free-depth solutions using clearly identifiable depth phases with depths determined by Cambridge using long-period *P* and *SH* body-wave modelling (1962–2005). (b) As a function of magnitude (1976–2005).

Comparison of EHB depths with Harvard CMT centroid depths

Another source of waveform-determined depths are Centroid Moment Tensor (CMT) solutions routinely determined by Harvard for events with moment magnitudes (M_w) greater than about 5.5. These solutions have been determined with long-period body and mantle waveform data using a moment tensor inversion method (for comprehensive summaries see Dziewonski *et al.* 1981; Dziewonski & Woodhouse 1983). The waveforms used are usually low-pass filtered at 45 s, and thereby lose sensitivity to depth for shallow crustal events. These wavelengths are considerably longer than those used in the *P* and *SH* body wave modelling described in the previous section, which have a peak sensitivity around 15 s period. Hypocentral parameters are obtained by adding perturbations resulting from the inversion to parameters reported by the USGS/NEIC. If the depth is not perturbed during the inversion, it is fixed to be consistent with the waveform matching of reconstructed broad-band body waves (Ekström 1989). Occasionally, a 'geophysicist' depth is applied, especially in continental regions where both the USGS/NEIC and CMT give dubious depths. In the absence of such detailed examination, default depths are 15 km (12 km now) and 33 km (10 km from 1981 to 1985). More recently, the CMT analysis has been extended to smaller earthquakes by analysing teleseismic intermediate-period surface waves (Arvidsson & Ekström 1998), but except for regions

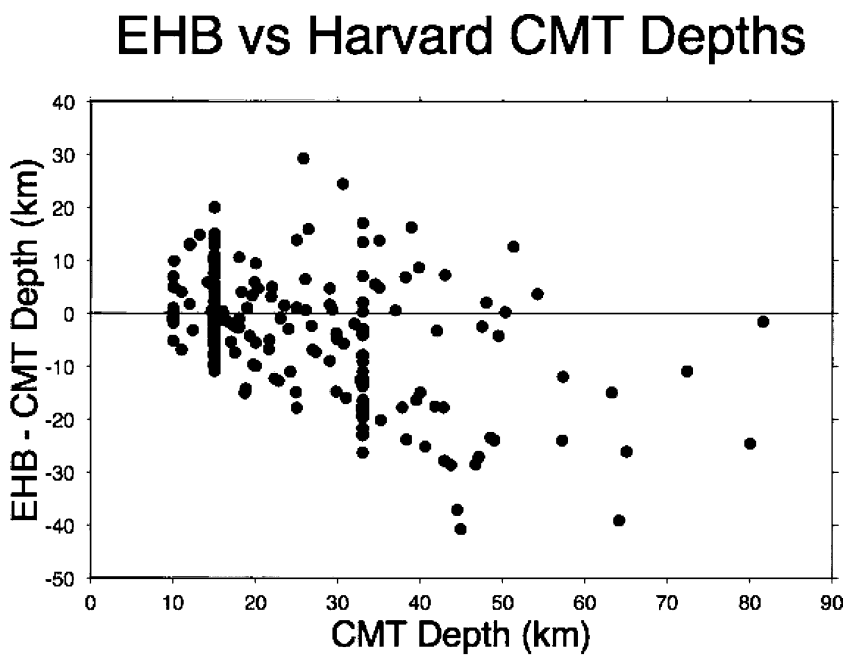

(a)

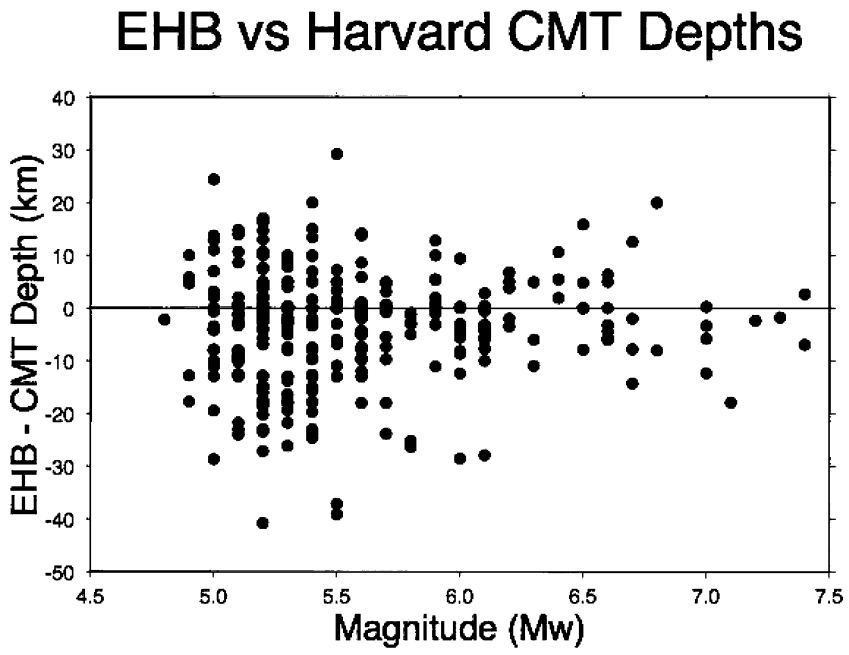

(b)

Figure 5. (a) Comparison of EHB free-depth solutions using clearly identifiable depth phases with CMT depths (1976–2004). (b) As a function of M_w magnitude (1976–2004).

with thick continental crust it is still no more sensitive to depth for shallow events.

The CMT data set provides an extremely valuable resource of focal mechanism data, but centroid depths lack the resolution to make meaningful comparisons with EHB depths (see Engdahl *et al.* 1998). Fig. 5(a) shows that differences between EHB hypocentres and CMT centroid depths are often quite large (median −3.8 km). Moreover, EHB depths for earthquakes where Harvard has used the default CMT depth of 33 km are nearly all shallower and within the crust in the ak135 model (<35 km). It is also obvious from Fig. 5(b) that the larger depth differences are associated with the smaller events, suggesting a CMT resolution problem for these more-poorly recorded earthquakes. Some of the discrepancies also may be related to the differences between the earth models used in EHB and CMT depth determinations. However, there is an obvious danger in making these comparisons for the largest events, as EHB locations are concerned with the nucleation point of the rupture, whereas the CMT locations represent the centroid of fault slip.

Confirmation of depth phases by using digital waveforms

The complexity of teleseismic *P* waves for Iranian events is recognized in previous studies (e.g. Baker *et al.* 1993; Maggi *et al.* 2000a). Maggi *et al.* (2000a) studied an earthquake that occurred on 1985 February 2 (20:52:32.48, 28.354N, 52.973E, 11.0). The first-arriving *P* wave was followed by another strong pulse that was called a depth phase in some analyses and not called anything at all in other analyses. In cases where the second arrival was called a depth phase, the depth was determined to be approximately 122 km. The CMT solution was a crustal-depth normal fault. Maggi *et al.* (2000a) modelled the *P* and *SH* seismograms, and found that this event is best explained with two thrust earthquakes at shallow depth. Determining the source parameters for this event required detailed analysis of the waveforms. Otherwise, the depth and the focal mechanism are anomalous for the region.

We further investigated select Zagros events by analysing broadband waveforms. As an example, in Fig. 6 we present *P*-wave seismograms recorded at six stations for an M_w 5.2 Zagros earthquake occurring on 1999 April 30 (04:19:59.46, 27.771N, 53.544E, 4.1). In each case there is a prominent secondary phase, which was widely reported in the ISC bulletin as a depth phase and in the IDC_REB catalogue with an *sP* phase assignment and a 43.8 km event depth. We overlay the 1st and second arrival in each seismogram by advancing the 2nd arrival by 17.4 s. Although each waveform samples a distinctly difference distance and azimuth from the event, there is good agreement between the waveforms. The consistent offset of the two pulses at widely ranging distances and azimuths suggest that the second pulse is not a depth phase, but instead is the result of a second moment release (second event) in close proximity and with a focal mechanism similar to that of the first event. Our analysis suggests that the depth phases for this event are contained within the *P*-wave pulse, which is not inconsistent with a revised depth for this event of 4.1 km independently determined by modelling InSAR ground displacement (Lohman & Simons 2005).

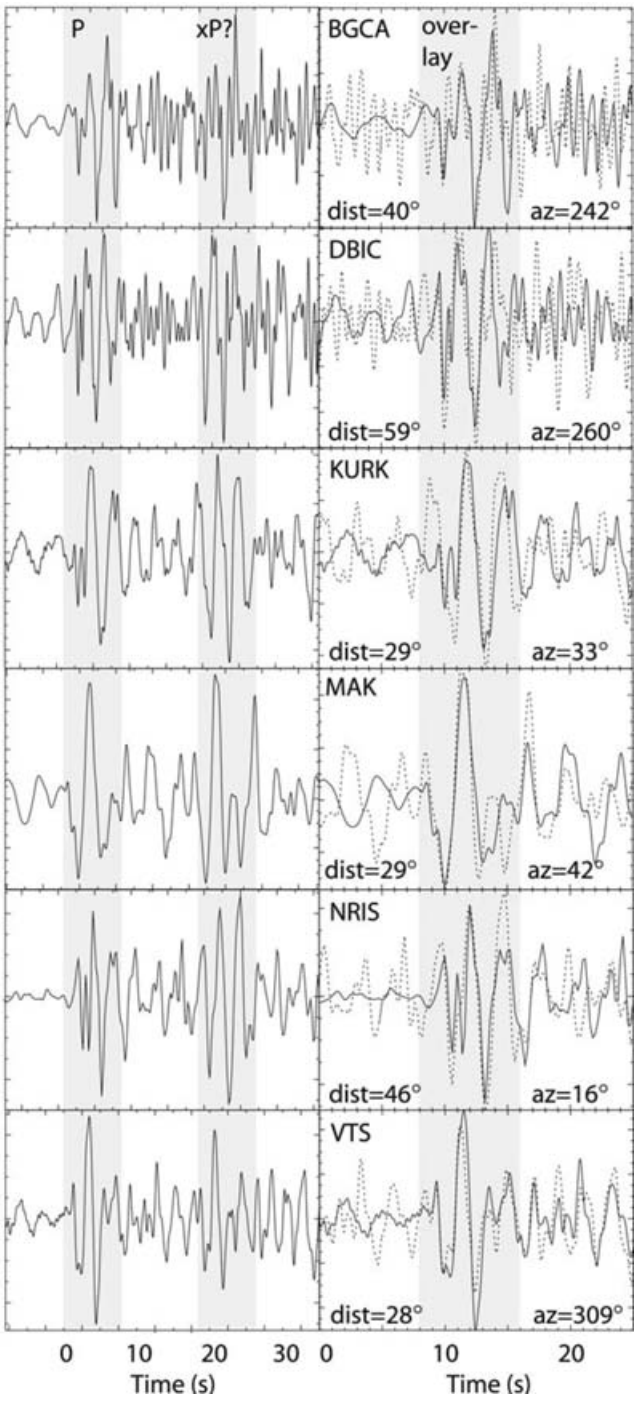

Figure 6. Seismograms for a 1999/04/30 Zagros event. Left column: broadband records with *P*-phase in light grey backdrop and the secondary phase picked as a depth phase in darker grey backdrop. Right column: overlay of *P*-phase (solid) and secondary phase (dash). In each case the secondary phase is advanced by 17.4 s. In each case the agreement between the two phases is excellent for a wide range of distances and azimuths, suggesting that the secondary phase is attributed to a second event (or doublet).

Summary: Assessment of EHB depths

Although EHB depth phase association and free-depth estimation ordinarily provide a reasonable fit to depth that often agree with independent estimates, problems are encountered when the starting depths are poor, there are too few depth phases and the procedure becomes unstable, or the earthquakes are complex. The problem with complex events is that sub-event arrivals are often confused with depth phases by the association algorithm so that there is no sensible fit. This problem is addressed by fixing the depth to an estimate that has been reliably determined for that earthquake by other means (e.g. from waveforms or InSAR studies). However, a poor starting depth or too few depth phases is a significant problem in EHB depth determinations and usually requires a careful review of the output of the automatic processing. Subsequently, the starting depth is adjusted or fixed in order to obtain a best fit to the reported depth phases in a new hypocentre solution. From the depth comparisons made previously we estimate that, after review, the uncertainties in our EHB depth estimates are $\pm$10 km. This agrees well with a separate independent study by Engdahl (2006) using a globally distributed data set of reference events (explosions and earthquakes) known in location and depth to 5 km or better. In that study, EHB procedures resulted in average formal free-depth uncertainties of $\pm$8 km, indicating depth-phase reading errors on the order of 1 s. The median formal depth uncertainty for all EHB free-depth solutions in the Iran region using depth phases is 3.7 $\pm$ 1.6 km, but this does not reflect the true depth accuracy, only the fit to the phase data.

RESULTS FOR IRAN

Regional distribution of seismicity

There are 2227 earthquakes that occurred in the Iran region that have well-constrained (secondary teleseismic azimuth gap <180 degrees) epicentres for the period 1918–2004 based on phase arrival times reported to the ISS, ISC and USGS/NEIC. Of these events, 1226 have depths estimated from EHB-associated depth phases or from waveforms (primarily during the post-1964 period). EHB events with unconstrained depths based on first arriving *P* arrival times alone are usually poorly determined and have been set to default depths based on the regional medians of nearby better determined depth estimates. This insures that, when other depth constraints for an event are not available, the use of an inappropriate depth does not unduly bias the relocated epicentre. The new locations for all events (colour coded by depth) are plotted in Fig. 7(a), along with known major faults compiled by Berberian & Yeats (1999) that have been updated by Richard Walker (personal communication). Fig. 7(b) is similar except only events having depths determined by *P* and *SH* body wave modelling are shown. The comparison is important because it shows the geographical coverage, and also reveals places where EHB depths do not have direct waveform confirmation and hence are particularly interesting for future earthquakes. Iran is presently one of the few areas in which this comparison can be made. Seismic-moment release for larger events, estimated by a logarithmic scaling of the seismic moment (M_0) using the formula $\log 10(M_0 - 22.25)$ Newton-metres, is plotted in Fig. 8. Major moment release is clearly evident in eastern and northern Iran, with many $M_w > 7$ events. The figure also shows a known result that the Zagros, although the source of frequent earthquakes of M_w 6.0–6.5, has a relatively low total moment release (Jackson & McKenzie 1988; Masson *et al.* 2005). Also plotted in Fig. 7(b) is a regionalization scheme for the Iran region largely based on tectonic style, as well as the distribution of seismicity, focal depths and seismic moment release. In the following sections we will assess the patterns of seismicity and depth distribution in each of the six regions shown.

Central Caspian region—offshore deep and onshore shallower seismicity

Earthquakes in this region occur over a wide range of depths (Fig. 9a) with a median depth of 40 ± 15 km, but this generalization hides a clear geographical pattern to the distribution of focal depths. A band of earthquakes crossing the central Caspian beneath the Apscheron–Balkhan sill and continuing onshore in the east into the Cheleken peninsular of Turkmenistan (Figs 1 and 7a) includes many earthquakes in the mantle, some as deep as 80 km but none shallower than 30 km. The deepest earthquakes are on the northern side of this zone, but there are an insufficient number of them to define a dipping mantle slab (Jackson *et al.* 2002). South of this trans-Caspian band, the South Caspian basin itself, surrounded by active earthquake belts (Fig. 1: Kopeh Dagh, Alborz and Talesh) on all sides, is apparently aseismic (Fig. 7a). Crustal thickness varies across the region. Receiver functions and Russian deep seismic sounding as well as surface wave analysis (Priestley *et al.* 2001), show that the crust in Turkmenistan east of the sill and north of the Kopeh Dagh is 45–50 km thick, and 30–35 km thick in the low-lying SE and SW onshore parts of the South Caspian basin. The offshore basin itself has at least 20 km of young sediment overlying a high-velocity basement that is either thicker than normal oceanic crust or thinned continental crust, whereas north of the Apscheron–Balkhan sill the crust is continental in character and 45–50 km thick (Mangino & Priestley 1998).

Given the uncertainty about the nature of the high-velocity basement beneath the thick sediments of the South Caspian basin, the events at depths between 30 and 50 km beneath the Apscheron–Balkhan sill, whose focal mechanisms show predominantly normal faulting with an ESE strike (Jackson *et al.* 2002), are difficult to interpret. The Apscheron–Balkhan sill is a prominent bathymetric feature separating the deep South Caspian basin from the shallower northern Caspian. The sill coincides with an anticline in the sediments of the Late Miocene–Early Pliocene productive series, but its deeper structure is not well imaged on seismic reflection profiles. Several events that lie on the north side of the sill between 70 and 80 km depth are clearly in the mantle, and are thought to represent either the last oceanic remnant of subduction of a now-closed ocean basin or the incipient NE subduction of the South Caspian basin basement beneath the sill (Priestley *et al.* 1994; Jackson *et al.* 2002). This subduction is a process that appears to occur aseismically at shallow depths, with the lack of earthquakes in the basin indicating that it behaves as a roughly $300 \times 300\,\mathrm{km}^2$ relatively rigid block within the Eurasia–Iran–Arabia collision zone. There is no evidence for seismicity deeper than 100 km, suggesting that the subduction is either slow or young (Jackson *et al.* 2002).

Alborz region—seismicity throughout the crust

Roughly 50 per cent of the $\sim$20 mm yr^{-1} N–S convergence between Arabia and Iran (Vernant *et al.* 2004) is accommodated in the Alborz region, between the southern Caspian and central Iran. Earthquakes in this region along the Alborz mountains and other southern Caspian basin active border regions to the SW, E occur at all depths in the crust (Fig. 9b) with a median depth of 20 ± 8 km. However, this generalization again hides a clear geographical variation in the known depths. Along the western side of the South Caspian basin, beneath the Talesh mountains of Iran (Fig. 1), earthquakes occur to depths of $\sim$30 km, generally on low-angle thrusts (based on available focal mechanism data), indicating underthrusting of the Caspian sea floor beneath the coast (Jackson *et al.* 2002). East of 50°E all waveform-modelled depths are shallower than 15 km (Jackson *et al.* 2002), but there are a few EHB depths of up to 35 km (Figs 7a and 9b). A receiver function result in the central Alborz mountains shows that the crust is $\sim$35 km thick, with a structure typical of continents (M. Tatar, personal communication, 2000). The western Alborz (the Talesh), with its low-angle underthrusting, is tectonically distinct from the central and eastern Alborz, which is dominated by strike-slip and high-angle reverse faulting at shallower depths (Fig. 7b).

Zagros region—seismicity mostly in the upper crust

The Zagros mountains of SW Iran form a linear intra-continental fold-and-thrust belt about 1200 km long, trending NW-SE between the Arabian shield and central Iran, with a width varying between 200 and 300 km. Roughly 50 per cent of the convergence rate between the Arabia Plate and the continental crust of central Iran is accommodated in the Zagros by north-south crustal shortening oblique to the strike of the belt over much of its length (Tatar *et al.* 2002; Vernant *et al.* 2004). Of particular interest is whether or not the earthquake depths in this region show any evidence for intra-continental subduction. In the Ghir region of the central-southern

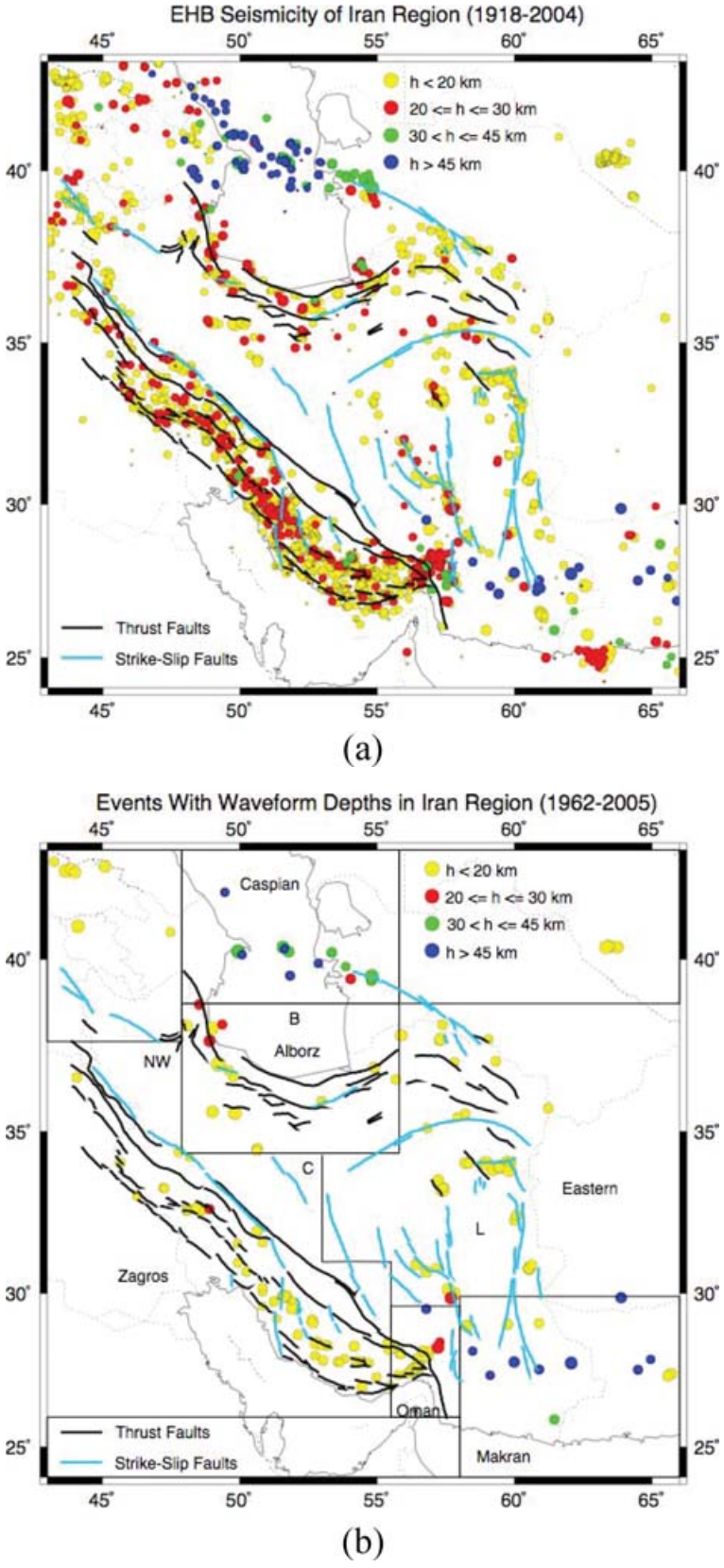

Figure 7. (a) EHB regionalized seismicity in the Iran region (1918–2004). Also shown are thrust (black) and strike-slip (blue) faults. (b) Regionalized seismicity in the Iran region for events with depths determined by *P* and *SH* body-wave modelling (1962–2004). Also shown are thrust (black) and strike-slip (blue) faults. The boxes outline the six regions (Caspian, Alborz, Zagros, Oman Line, Makran and Eastern) in which the patterns of seismicity and depth distribution will be discussed. Relatively aseismic and rigid blocks in the South Caspian basin (B), Dasht-e-Lut (L), central Iran (C) and NW Iran (NW), surrounded by seismically active mountain belts, are also indicated.

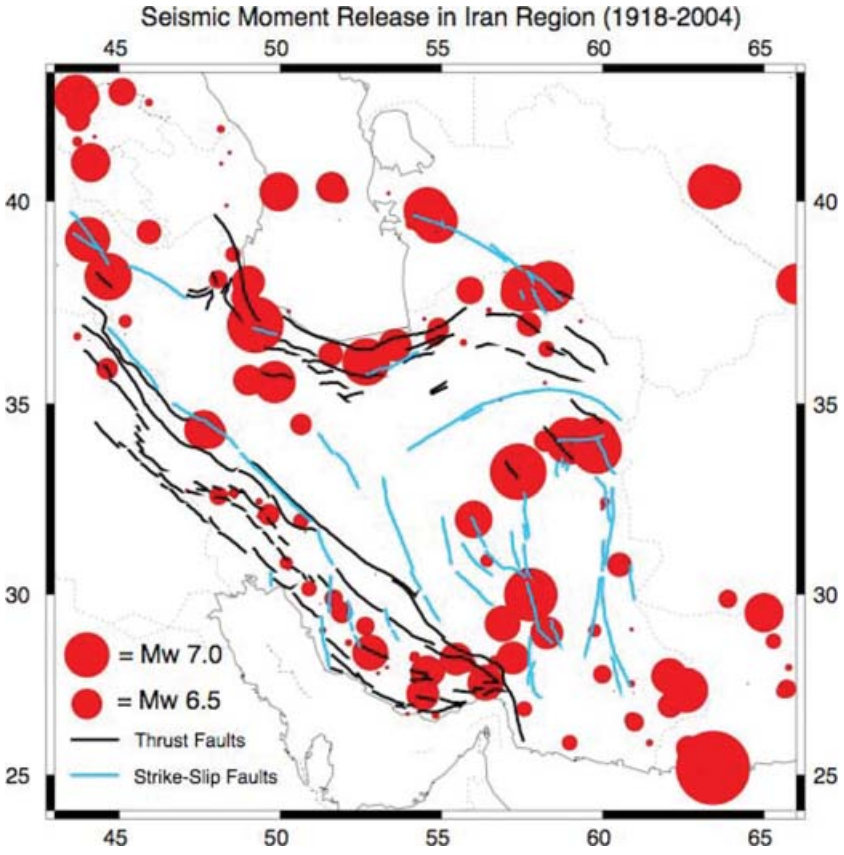

Figure 8. Seismic moment release in the Iran region (1918–2004). Scaling by equivalent moment magnitude (M_w) is indicated.

Zagros, Hatzfeld *et al.* (2003) found, based on a microearthquake survey and receiver functions, a crustal structure consisting of an ∼11 km thick sedimentary layer overlying an ∼35 km thick crystalline crust. The crystalline crust consists of an upper layer extending from ∼11 to 19 km depth and a lower layer extending from ∼19 km depth, to a crust-mantle interface at ∼46 km depth. Moreover, in that region most well-located microearthquakes occurred between 10 and 14 km depth, with none occurring deeper than 20 km (Tatar *et al.* 2004). In their review of waveform-modelled depths in the Zagros, Talebian & Jackson (2004) found no earthquakes deeper than 20 km anywhere except near the Oman Line in the extreme SE Zagros (discussed in the next section). In the revised EHB database presented here, nearly all earthquakes in the Zagros are less than 30 km in depth (Fig. 9c), a result consistent, given the expected uncertainty of 10 km, with the above-mentioned microearthquake and waveform-modelled data. The median depth in Fig. 9(c) is 15 ± 7 km. However, EHB depths may be slightly overestimated in this region because of slower velocities at depth-phase bounce points in comparison with the faster crustal velocities of the ak135 model. Moreover, with a 10 km uncertainty in EHB depth estimates, most of these events probably occur within the upper crystalline crust but beneath the sedimentary layer. Hence, beneath the Zagros there is no evidence in the form of mantle earthquakes for present-day active subduction of continental crust, with shortening apparently accommodated entirely by crustal thickening and distributed deformation (Talebian & Jackson 2004). Finally, the Zagros has many earthquakes, but their magnitudes are all less than M_w 7.0 and nearly all the moment release occurs near the SW topographic edge (i.e. elevations between 500–1000 m) of the belt (Fig. 8), (Talebian & Jackson 2004). Smaller earthquakes occur throughout the range. Numerous authors have pointed out that there is insufficient moment release in the Zagros to account for the expected convergence across it (most recently Masson *et al.* 2005), suggesting that the missing moment release is accommodated aseismically.

Oman Line region—transition from shallow Zagros to subcrustal Makran seismicity

The Oman Line is a geological syntaxis, where the faults and folds of the Zagros bend dramatically to connect with those of the Makran. The region is a transition from the continent-continent collision of the Zagros to the subduction of the Arabian plate beneath the Makran coast, and is geologically complex (e.g. Molinaro *et al.* 2004; Regard *et al.* 2004, 2005). GPS measurements indicate N–S convergence between Oman and central Iran of about 11 mm yr^{-1} (Vernant *et al.* 2004), expressed as a mixture of shortening and N–S right-lateral strike-slip on the eastern side of the syntaxis. In the west and central part of the syntaxis, waveform modelling shows earthquakes increasing in depth northwards, from typically 8–12 km near the coast to as much as 28 km at a location 50 km north of the geological suture (the Main Zagros Thrust) that represents the join between Arabian and Iranian rocks (Talebian & Jackson 2004). The deepest earthquakes are all low-angle thrusts, dipping gently northwards, and represent one of the few places where a case can be made for underthrusting of Arabian basement beneath central Iran; but only by a distance of 50 km to a depth of ∼30 km. The eastern limit of the Oman Line region in Fig. 7(b) is drawn so as to exclude most of the Makran subduction zone, but one waveform-modelled earthquake at 100 km depth (Maggi *et al.* 2000a) is included in its

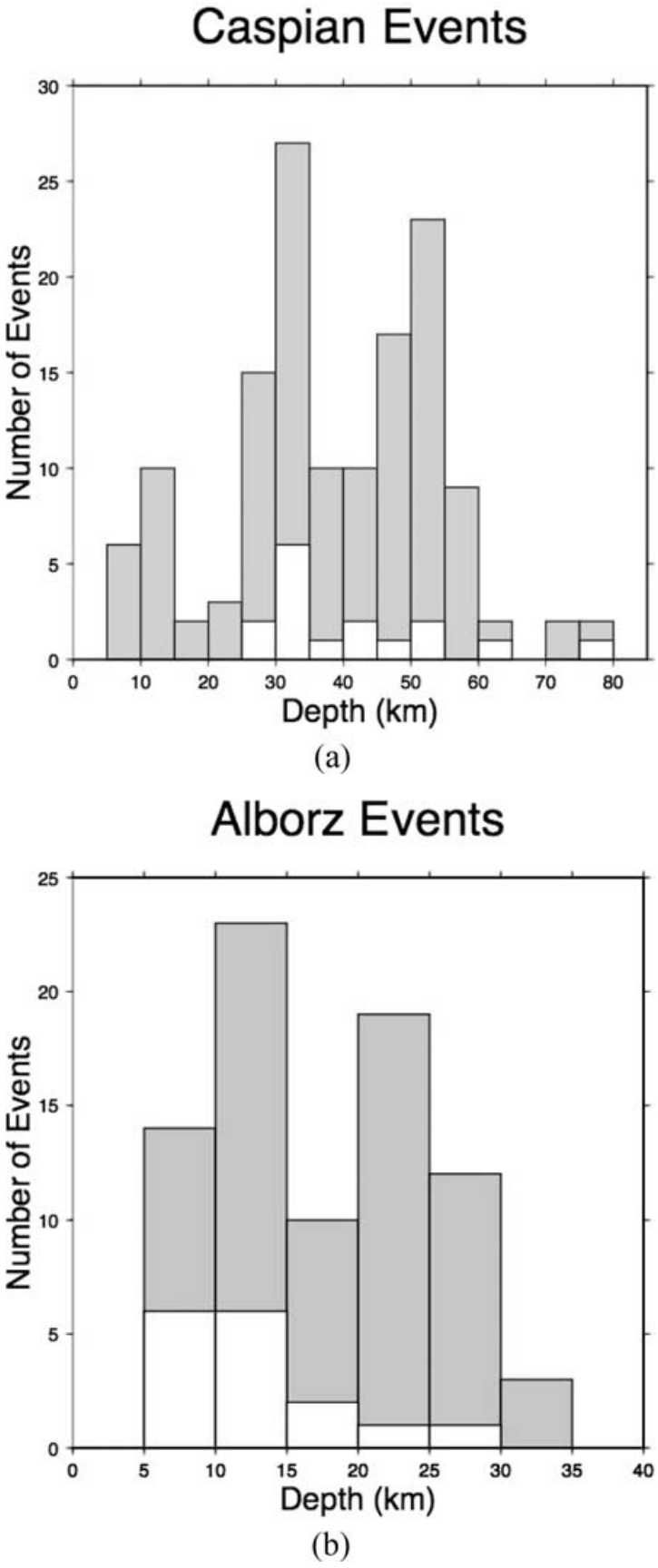

Figure 9. Earthquake depth distribution by region (depths determined by waveform modelling are not shaded). (a) Caspian, (b) Alborz, (c) Zagros, (d) Oman Line, (e) Makran and (f) Eastern.

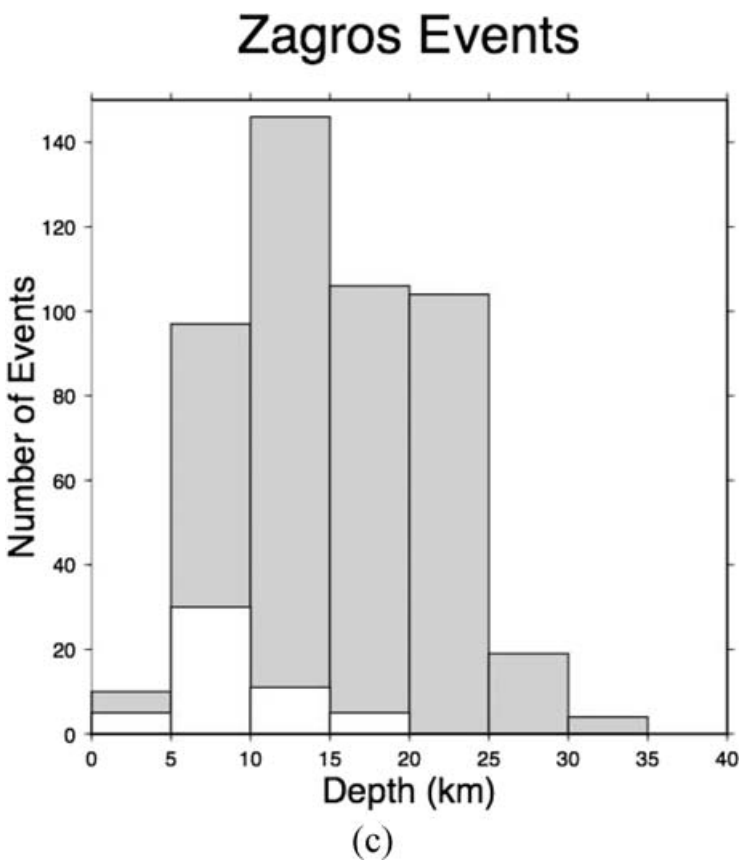

(c)

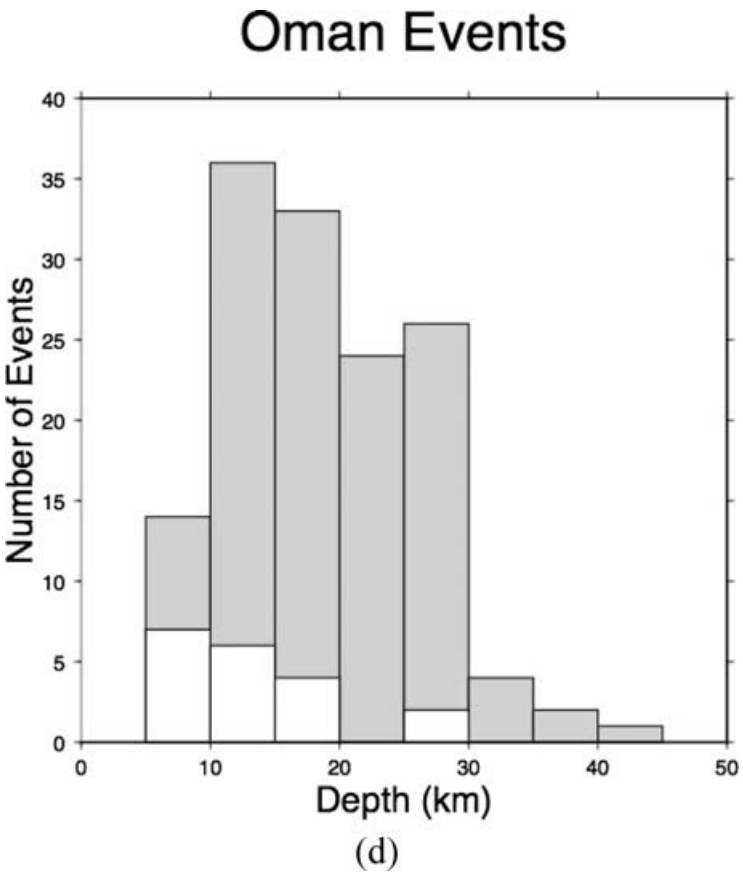

(d)

Figure 9. (*Continued*.)

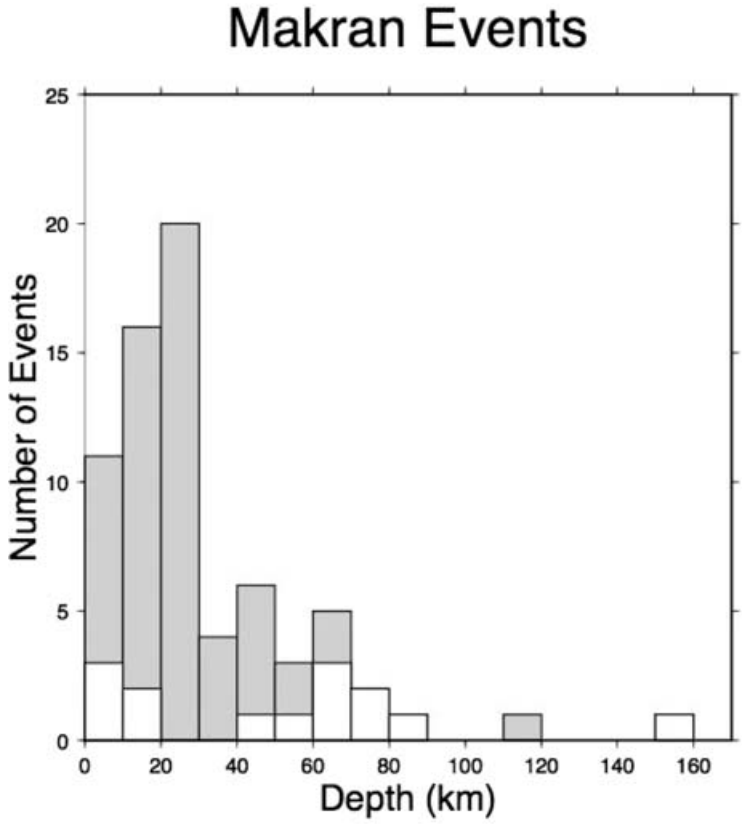

(e)

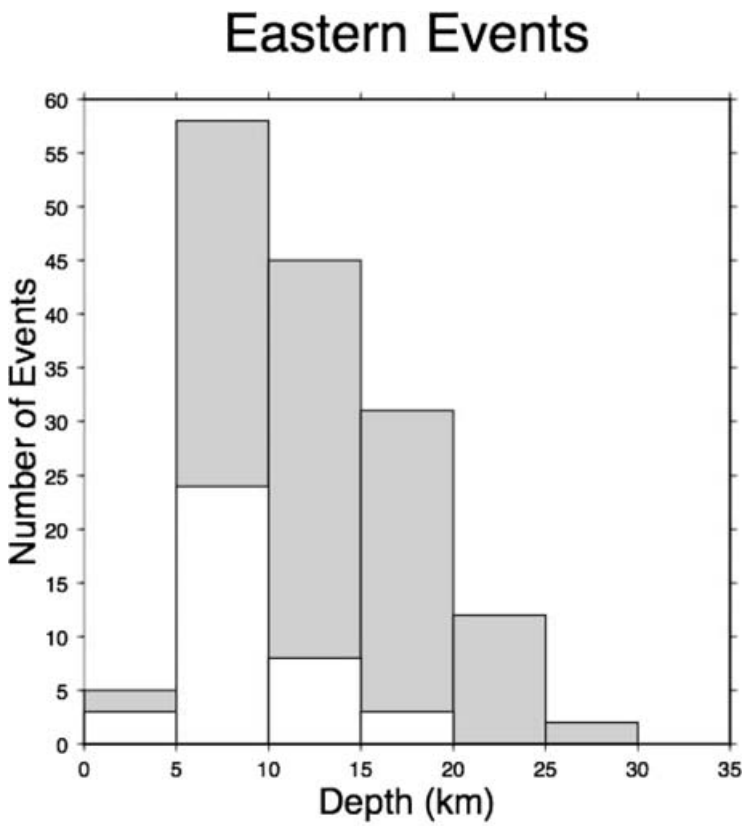

(f)

Figure 9. (*Continued*.)

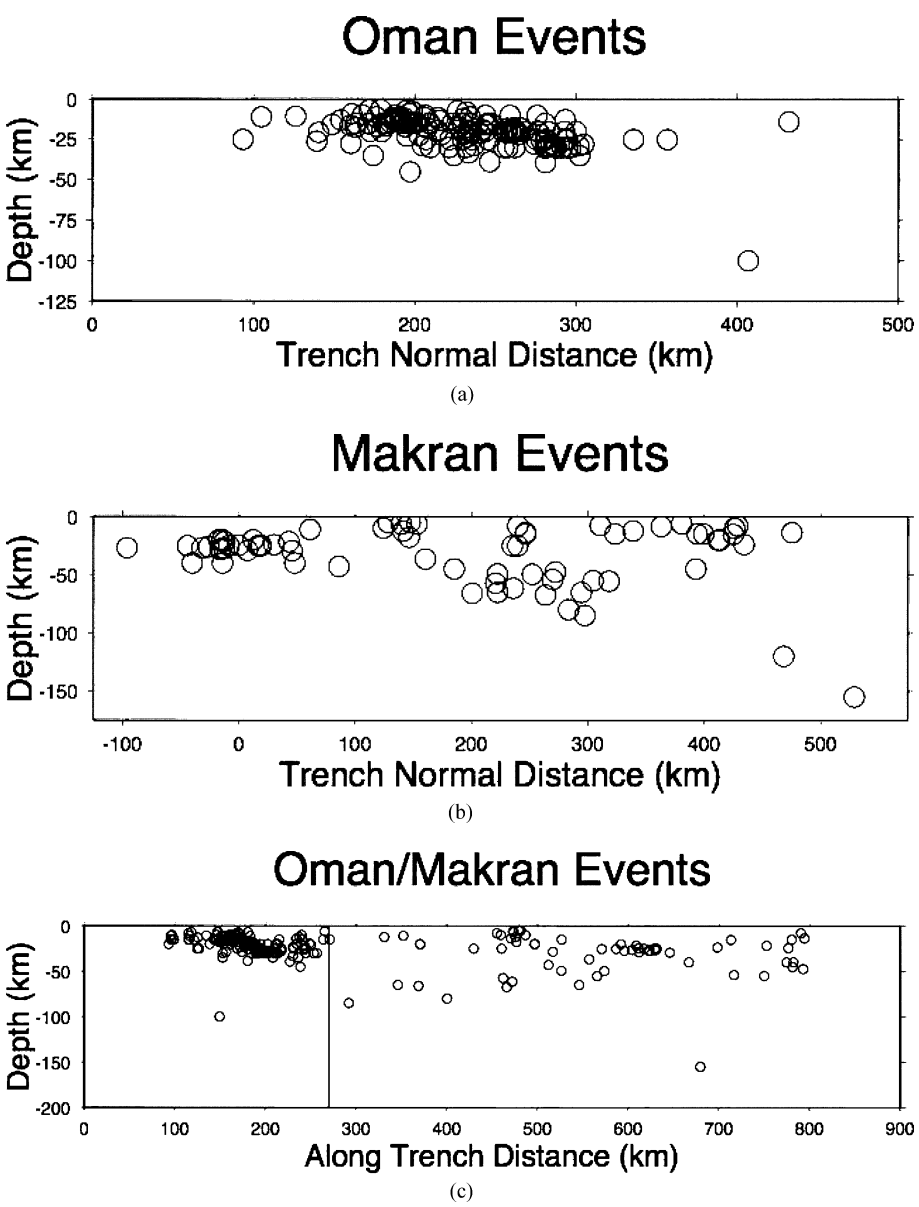

Figure 10. Cross sections (no vertical exaggeration) at distances with respect to a centre of curvature of the Makran trench at 46.131N and 63.172E. (a) Earthquakes in Oman Line region of Fig. 7 plotted normal to the trench. (b) Earthquakes in the Makran region of Fig. 7 plotted normal to the trench. (c) Earthquakes in the Oman Line and Makran regions of Fig. 7 plotted along trench strike.

northern part. EHB seismicity within the box extends to depths of about 40 km (Figs 9d and 10a), consistent with the waveform data summarized above, with a median depth of 20 ± 8 km. The EHB data set contains earthquakes on the eastern side of the syntaxis at 30–40 km (Fig. 7a), but these have not been confirmed by waveform modelling.

Makran region—low-level, upper-crustal and subduction-related mantle seismicity

East of 57.3°E, most of the ∼30 mm yr^{-1} shortening produced by Arabia-Eurasia convergence is accommodated by the Makran subduction zone (Vernant *et al.* 2004). The Makran region has earthquakes both at upper crustal depths and at depths well in excess of 40 km (Fig. 9e) with a median depth of 25 ± 19 km. The deeper events apparently occur within a shallow (∼26°) northward dipping slab (Fig. 10b), confirming the tectonic views of Jackson & McKenzie (1984), Laana & Chen (1989) and Byrne *et al.* (1992). These mantle-depth events in the Makran result from the subduction of the Indian ocean beneath the relatively stable Lut and Afghan continental blocks, which joined in Eocene times. The Afghan block east of 60°E is now effectively part of undeforming Eurasia, separated from the Lut by the N–S right-lateral Sistan shear zone (Walker & Jackson 2004). Makran subduction seismicity is evident in Fig. 10(b), but the image (due to low seismicity rate) is not sharp. Most of the deeper events have down-dip T axes (Byrne *et al.* 1992; Maggi *et al.* 2000a), which is common in slabs that only extend about 200 km in depth (Isacks & Molnar 1971). An along-strike plot of seismicity (Fig. 10c) shows how earthquakes in the Oman Line zone merge at ∼57.3°E into lower-level seismicity beneath the Makran coastal ranges.

Eastern Iran—upper crustal seismicity surrounding the aseismic Lut and central Iran blocks

Seismicity in eastern Iran mostly surrounds the stable aseismic blocks of central Iran (Fig. 7a). North-south right-lateral shear between central Iran and Afghanistan is about 10–12 mm yr^{-1} (Vernant *et al.* 2004), mostly accommodated by N–S strike-slip faults on the east and west sides of the Lut block. It is probable that most of this shear occurs on the eastern side, whereas north of the Lut the shear is taken up by E–W left-lateral faults that rotate clockwise (Walker & Jackson 2004). The shear eventually ends as shortening against the Turkmenistan platform in the Kopeh Dagh range of NE Iran (Fig. 1). This whole region has been the source of many large earthquakes, many producing surface rupture, in both modern and historic times (Fig. 8; Ambraseys & Melville 1982; Walker & Jackson 2004). Earthquakes with waveform-modelled depths are all shallower than ∼20 km in this region, a pattern seen also in the larger EHB database (Figs 7 and 9f) which has a median depth of 12 ± 5 km.

One curiosity is worth pointing out. Aftershocks of the 2003 Bam earthquake, on the SW side of the Lut block, occurred in the restricted depth range 8–20 km (Tatar *et al.* 2005), whereas the mainshock itself (M_w 6.6) is known, from InSAR studies, to have ruptured only shallower than 8 km. Further north along the same fault system (the Gowk fault), earthquakes in 1981 appeared to also occur with waveform-modelled depths up to 20 km, with the same faults rupturing again at shallower levels in 1998 (Berberian *et al.* 2001). Not only is the seismogenic zone in this particular region relatively thick for Iran, but also it appears to be capable of rupturing its upper and lower parts in separate events. The implications of this are discussed further in Jackson *et al.* (2006).

DISCUSSION

The principal aim of this paper has been to present, and assess, the best catalogue of seismicity in the Iran region for the period 1918–2002 that we are able to assemble. The benefits and uses of this catalogue concern both epicentres and focal depths.

The EHB methodology, including the use of as many phases as is reasonable, with a modern (but still spherically symmetrical) velocity model, produces the best epicentres that are possible with any semi-routine location procedure. Careful calibration of these epicentres against known control events, for which the epicentre can be constrained by InSAR analysis or local seismic networks (e.g. Talebian *et al.* 2006), leads us to expect an location uncertainty of about 10 km, at least in the modern (post-1964) period. In spite of fewer stations and more timing errors, the accuracy of redetermined epicentres during the pre-1964 period is almost as good and a significant improvement on the old ISS locations (Ambraseys 1978; Berberian 1979). These improved epicentres, and knowledge of their uncertainty, represent a substantial advance in Iranian seismology and tectonics. For instance, earthquakes of M_w 6–6.5, with source dimensions of 10–20 km, are common in Iran; epicentres with errors of 10–20 km, uncritically or unknowingly used, can easily lead to an association of the earthquake with the wrong fault.

A principal concern of this paper has been focal depths. The depths we trust most are those that can be confirmed by waveform modelling; but they are necessarily limited to those earthquakes that are large enough to generate the long-period body waves for which the source appears as a simple centroid and, therefore, there are not many of them (167). In this study we have greatly enlarged the catalogue of depths that we believe to be reliable by including those determined from arrival times, but subject to stringent quality control, including the incorporation of reported *pP-P* and *sP–P* times and some checking of waveforms by inspection. This approach is not always foolproof, because surface reflections can be mis-identified, but the result is a catalogue that is homogeneous in its method of assessment and which, for the modern (post-1964) period, we believe is likely to have uncertainties of about 10 km in depth. This, again, is a substantial advance, since uncritically assessed routine catalogue depths are known to be uncertain by several tens of km. For geological or tectonic purposes, an uncertainty of tens of km in depths means we are unable to determine whether an earthquake was in the crust or mantle, and even less distinguish upper crust from lower crust or sedimentary cover. An important result of this study is that the EHB catalogue here (within its 10 km uncertainty) shows patterns that are consistent with the smaller number of waveform-modelled depths (within their lower uncertainty of about 4 km). The distribution of focal depths within Iran varies geographically, but correlates with the tectonic environment in a way that is informative.

In addition to their geological and tectonic significance, earthquake depth distributions have long been used to infer the relative variation of rhelogical properties within the lithosphere (e.g. Brace & Byerlee 1970; Chen & Molnar 1983; Wiens & Stein 1983). Maggi *et al.* (2000b) and Jackson *et al.* (2004), in a reassessment of waveform-modelled focal depths concluded that the continents show two behaviours; places where earthquakes are restricted to the upper crust (i.e. <20 km, including nearly all active regions today), and those where earthquakes occur throughout the crust (mostly associated with older Precambrian shield regions). They found little evidence for earthquakes in the continental mantle, and it seems that the mantle is seismogenic, in both oceans and continents, only when it is colder than about 600°C (McKenzie *et al.* 2005). There is nothing in the reassessed EHB catalogue presented here for Iran to contradict those views. Most crustal earthquakes in Iran are shallower than 20 km, though some are as deep as 30 km (e.g. in the Talesh, Cheleken and SE Zagros). Most of these would qualify as being in the 'upper crust', though the terminology is of questionable significance where sediments are very thick, as in the Zagros (up to ∼10 km in places) and in the southern Caspian and Cheleken (up to ∼20 km). Even where the earthquakes are as deep as 30 km, the crust may be considerably thicker (reaching greater than 50 km NE of the Zagros suture; Paul *et al.* 2006). Earthquakes that are definitely in the mantle are either certainly (in the Makran) or probably (in the central Caspian) within lithosphere of oceanic origin.

As a result of this study, we now have, for the first time, a coherent and consistent picture of how focal depth distributions vary geographically within Iran. This gives us clear expectations of what to expect in the future, and will allow us to readily identify apparently anomalous events for further checking and analysis. This situation is uncommon outside countries with permanent, dense networks of seismic stations (such as Japan and California).

CONCLUSIONS

We have relocated Iranian earthquakes occurring between 1918 and 2004. The image of seismic activity occurring at the boundaries between distinct tectonic blocks is sharpened, and—most significantly—event depths are refined. ISC locations throughout Iran (especially in the Zagros) tend to be in the lower crust or upper mantle. Our results suggest that the vast majority of Iranian events occur in the upper crust. Lower crustal locations are confirmed in the Oman Line and Alborz regions. Mantle events are associated

with the Makran subduction zone and in remnant subduction north of the southern Caspian Sea. Iranian seismicity is the result of the early stages of continent/continent collision between the Arabian Peninsula and Eurasia. Distinct tectonic blocks are responding to the nascent collision through relative motion, resulting in seismicity at the boundaries. Areas of heightened strain (collision with the Oman Peninsula and drastic variations in crustal structure around the southern Caspian) result in lower crustal seismicity. Finally, these results serve to illustrate the need to carefully reassess the reliability of catalogue-based depths before using them for geological, tectonic or even seismic-hazard purposes.

A compressed hypocentre data file (IRAN.HDF.gz) of relocated earthquakes occurring in the Iran region during the period 1918–2004 and a format description (FORMAT.HDF) can be retrieved by e-mail request to the first author at engdahl@colorado.edu.

ACKNOWLEDGMENTS

We are grateful to scientists at the Geological Survey of Iran, the International Institute of Earthquake Engineering and Seismology, and the University of Tehran, Institute of Geophysics, for support and research in Iran and for many helpful discussions. The ISC provided the phase arrival time data for 1964–2003, and the USGS/NEIC for 2004. Figures and maps were prepared using GMT (Wessel & Smith 1998). Comments by M. Anderson and M. Talebian improved the manuscript.

REFERENCES

Ambraseys, N.N., 1978. The relocation of the epicentres in Iran, *Geophys. J. R. astr. Soc.,* **53,** 117–121.

Ambraseys, N.N. & Melville, C.P., 1982. *A history of Persian earthquakes*, Cambridge University Press, UK, 219 p.

Arvidsson, R. & Ekström, G., 1998. Global CMT analysis of moderate earthquakes, $M_w \geq 4.5$, using intermediate period surface waves, *Bull. seism. Soc. Am.,* **88,** 1003–1013.

Baker, C., Jackson, J. & Priestley, K.F., 1993. Earthquakes on the Kazerun line in the Zagros Mountains of Iran: strike–slip faulting within a fold-and-thrust belt, *Geophys. J. Int.,* **115,** 41–61.

Berberian, M., 1979. Evaluation of instrumental and relocated epicentres of Iranian earthquakes, *Geophys. J. R. astr. Soc.,* **58,** 625–630.

Berberian, M. & Yeats, R.S., 1999. Patterns of historical earthquake rupture in the Iranian Plateau, *Bull. seism. Soc. Am.,* **89,** 120–139.

Berberian, M. *et al.*, 2001. The March 14 1998 Fandoqa earthquake (M_w 6.6) in Kerman province, SE Iran: re-rupture of the 1981 Sirch earthquake fault, triggering of slip on adjacent thrusts, and the active tectonics of the Gowk fault zone, *Geophys. J. Int.,* **146,** 371–398.

Bijwaard, H., Spakman, W. & Engdahl, E.R., 1998. Closing the gap between regional and global travel time tomography, *J. geophys. Res.,* **103,** 30 055–30 078.

Bird, P., Toksoz, M. & Sleep, N., 1975. Thermal and mechanical models of continent-continent convergence zones, *J. geophys. Res.,* **80,** 4405–4416.

Bolt, B.A., 1960. The revision of earthquake epicentres, focal depths and origin times using a high-speed computer, *Geophys. J. R. astr. Soc.,* **3,** 433–440.

Bondár, I., Myers, S.C., Engdahl, E.R. & Bergman, E.A., 2003. Epicentre accuracy based on seismic network criteria, *Geophys. J. Int.,* **156,** 483–496.

Brace, W.F. & Byerlee, J.D., 1970. California earthquakes: why only shallow focus?, *Science,* **168,** 1573–1576.

Byrne, D.E., Sykes, L.R. & Davies, D.M., 1992. Great thrust earthquakes and aseismic slip along the plate boundary of the Makran subduction zone, *J. geophys. Res.,* **97,** 449–478.

Chen, W.-P. & Molnar, P., 1983. Focal depths of intracontinental earthquakes and intraplate earthquakes and their implications for the thermal and mechanical properties of the lithospheric evolution, *J. geophys. Res.,* **88,** 4183–4214.

Choy, G.L. & Engdahl, E.R., 1987. Analysis of broadband seismograms from selected IASPEI events, *Phys. Earth planet. Inter.,* **47,** 80–92.

Choy, G.L. & Dewey, J.W., 1988. Rupture process of an extended earthquake sequence: Teleseismic analysis of the Chilean earthquake of 3 March 1985, *J. geophys. Res.,* **93,** 1103–111.

Dziewonski, A.M. & Woodhouse, J.H., 1983. Studies of the seismic source using normal-mode theory, in edsKanamori, H. & Boschi, E., Earthquakes: observation, theory, and interpretation: notes from the International School of Physics 'Enrico Fermi' (1982: Varenna, Italy), North-Holland Publ. Co., Amsterdam, The Netherlands, pp. 45–137.

Dziewonski, A.M., Chou, T. & Woodhouse, J.H., 1981. Determination of earthquake source parameters from waveform data for studies of global and regional seismicity, *J. geophys. Res.,* **86,** 2825–2852.

Ekström, G., 1989. A very broad band inversion method for the recovery of earthquake source parameters, *Tectonophysics,* **166,** 73–100.

Engdahl, E.R., 2006. Application of an improved algorithm to high-precision teleseismic relocation of ISC test events, *Phys. Earth planet. Int.,* doi:10.1016/j.pepi.2006.03.007.

Engdahl, E.R. & Gunst, R.H., 1966. Use of a high speed computer for the preliminary determination of earthquake hypocenters, *Bull. seism. Soc. Am.,* **56,** 325–336.

Engdahl, E.R. & Bergman, E.A., 2001. Validation and generation of reference events by cluster analysis, *23rd Seismic Research Review*, Jackson Hole. http://www.cmr.gov/srs/srs2001/Screen/ 02–09.pdf.

Engdahl, E.R. & Villasenor, A., 2002. *Global Seismicity: 1900–1999, International Handbook of Earthquake and Engineering Seismology, v*. 81A, Elsevier Science Ltd., Amsterdam, The Netherlands, pp. 665–690.

Engdahl, E.R., Van der Hilst, R.D. & Buland, R.P., 1998. Global teleseismic earthquake relocation with improved travel times and procedures for depth determination, *Bull. seism. Soc. Am.,* **88,** 722–743.

Harvey, D. & Choy, G.L., 1982. Broadband deconvolution of GDSN data, *Geophys. J. R. astr. Soc.,* **69,** 659–668.

Hatzfeld, D., Tatar, M., Priestley, K. & Ghafory-Ashtiany, M., 2003. Seismological constraints on the crustal structure beneath the Zagros Mountain belt (Iran), *Geophys. J. Int.,* **155,** 403–410.

Isacks, B. & Molnar, P., 1971. Distribution of stresses in the descending lithosphere from a global survey of focal mechanism solutions of mantle earthquakes, *Rev. Geophys. Space Phys.,* **9,** 103–174.

Jackson, J.A. & McKenzie, D.P., 1984. Active tectonics of the Alpine– Himalayan belt between western Turkey and Pakistan, *Geophys. J. R. astr. Soc.,* **77,** 185–264.

Jackson, J.A. & McKenzie, D., 1988. The relationship between plate motions and seismic moment tensors, and the rates of active deformation in the Mediterranean and Middle East, *Geophys. J.,* **93,** 45–73.

Jackson, J., Priestley, K., Allen, M. & Berberian, M., 2002. Active tectonics of the South Caspian basin. *Geophys. J. Int.,* **148,** 214–245.

Jackson, J., Austrheim, H., McKenzie, D. & Priestley, K., 2004. Metastability, mechanical strength and the support of mountain belts, *Geology,* **32,** 625–628.

Jackson, J. *et al.*, 2006. Seismotectonic, rupture-process, and earthquake-hazard aspects of the 2003 December 26 Bam, Iran, earthquake, *Geophys. J. Int.,* **166,** 1270–1292.

Jeffreys, H. & Bullen, K.E., 1940. 'Seismological Tables'. British Association for the Advancement of Science, London.

Kennett, B.L.N. & Engdahl, E.R., 1991. Traveltimes for global earthquake location and phase identification. *Geophys. J. Int.,* **105,** 429–465.

Kennett, B.L.N. & Gudmundsson, O., 1996. Ellipticity corrections for seismic phases, *Geophys. J. Int.,* **127,** 40–48.

Kennett, B.L.N., Engdahl, E.R. & Buland, R., 1995. Constraints on seismic velocities in the Earth from traveltimes, *Geophys. J. Int.,* **122,** 108–124.

Laana, J.L. & Chen, W.-P., 1989. The Makran earthquake of 1983 April 18: a possible analogue to the Puget Sound earthquake of 1965? *Geophys. J. Int.,* **98,** 1–9.

Lohman, R.B. & Simons, M., 2005. Locations of selected small earthquakes in the Zagros Mountains, *Geochem. Geophys. GeoSys.,* **6**, doi:10.1029/2004GC000849.

Maggi, A., Jackson, J.A., Priestley, K. & Baker, C., 2000a. A re-assessment of focal depth distributions in southern Iran, the Tien Shan and northern India: do earthquakes really occur in the continental mantle?, *Geophys. J. Int.,* **143,** 629–661.

Maggi, A., Jackson, J.A., McKenzie, D. & Priestley, K., 2000b. Earthquake focal depths, effective elastic thickness, and the strength of the continental lithosphere, *Geology,* **28,** 495–498.

Maggi, A., Priestley, K. & Jackson, J.A., 2002. Earthquake focal depths in the Iran region, *J. Seismology and Earthquake Engineering,* **4,** 1–10.

Mangino, S. & Priestley, K., 1998. The crustal structure of the southern Caspian region, *Geophys. J. Int.,* **133,** 630–648.

Masson, F., Chery, J., Hatzfeld, D., Martinod, J., Vernant, P., Tavakoli, F. & Ghafory-Ashtiani, M., 2005. Seismic versus aseismic deformation in Iran inferred from earthquakes and geodetic data, *Geophys. J. Int.,* **160,** 217–226.

McKenzie, D., Jackson, J. & Priestley, K., 2005. Thermal structure of oceanic and continental lithosphere, *Earth. planet. Sci. Lett.,* **233,** 337–349.

Molinaro, M., Guezou, J.C., Leturney, P., Eshaghi, S.A. & de Lamotte, D.F., 2004. The origin of changes in structural style across the Bandar Abbas syntaxis, SE Zagros (Iran), *Mar. Pet. Geolo.,* **21,** 735–752.

Myers, S.C. & Schultz, C.A., 2000. Calibration of seismic travel time using events with seismically determined locations and origin times, *EOS, Trans. Am. geophys. Un.,* **81,** F845.

Niazi, M., Asudeh, I., Ballard, G., Jackson, J.A., King, G. & McKenzie, D.P., 1978. The depth of seismicity in the Kermanshah region of the Zagros Mountains (Iran), *Earth planet. Sci. Lett.,* **40,** 270–274.

Nowroozi, A.A, 1971. Seismotectonics of the Persian plateau, eastern Turkey, Caucasus, and Hindu Kush regions, *Bull. seism. Soc. Am.,* **61,** 317–341.

Paul, A., Kaviani, A., Hatzfeld, D.S., Vergne, J. & Mokhtari, M., 2006. Seismological evidence for crustal-scale thrusting in the Zagros mountain belt (Iran), *Geophys. J. Int.,* **166,** 277–237.

Priestley, K., Patton, H. & Scholz, C., 2001. Modelling anomalous surface-wave propagation across the Southern Caspian Basin, *Bull. seism. Soc. Am.,* **91,** 1924–1929.

Priestley, K., Baker, C. & Jackson, J., 1994. Implications of earthquake focal mechanism data for the active tectonics of the south Caspian Basin and surrounding regions, *Geophys. J. Int.,* **118,** 111–141.

Regard, V., Bellier, O., Thomas, J-C., Abrassi, M.R., Mercier, J., Shabanian, E., Fegghi, K. & Soleymani, S., 2004. Accommodation of Arabia-Eurasia convergence in the Zagros-Makran transfer zone, SE Iran: a transition between collision and subduction through a young deforming system, *Tectonics,* **23,** TC4007.

Regard, V. *et al.*, 2005. Cumulative right-lateral fault slip rate across the Zagros-Makran transfer zone: role of the Minab-Zendan fault system in accommodating Arabia-Eurasia convergence in southeast Iran, *Geophys. J. Int.,* **162,** 177–203.

Talebian, M. & Jackson, J., 2004. A reappraisal of earthquake focal mechanisms and active shortening in the Zagros mountains of Iran, *Geophys. J. Int.,* **156,** 1–21.

Talebian, M. *et al.*, 2006. The Dahuiyeh (Zarand) earthquake of 2005 February 22 in central Iran: reactivation of an intramountain reverse fault, *Geophys. J. Int.,* **164,** 137–148.

Tatar, M., Hatzfeld, D., Martinod, J., Walpersdorf, A., Ghafory-Ashtiany, M. & Chery, J., 2002. The present-day deformation of the central Zagros from GPS measurements, *Geophys. Res. Lett.,* **29**, doi:10.1029/2002GL015159.

Tatar, M., Hatzfeld, D. & Ghafory-Ashtiany, M., 2004. Tectonics of the Central Zagros (Iran) deduced from microearthquake seismicity, *Geophys. J. Int.,* **156,** 255–266.

Tatar, M., Hatzfeld, D., Moradi, A.S. & Paul, A., 2005. The 2003 December 26 Bam earthquake (Iran), M_w 6.6 aftershock sequence, *Geophys. J. Int.,* **163,** 90–105.

van der Hilst, R.D. & Engdahl, E.R., 1992. Step-wise relocation of ISC earthquake hypocenters for linearized tomographic imaging of slab structure, *Phys. Earth planet. Int.,* **75,** 39–54.

Vernant, P. *et al.*, 2004. Present-day crustal deformation and plate kinematics in the Middle East constrained by GPS measurements in Iran and northern Oman, *Geophys. J. Int.,* **157,** 381–398.

Walker, R. & Jackson, J., 2004. Active tectonics and Late Cenozoic strain distribution in central and eastern Iran, *Tectonics,* **23**, doi:10.1029/2003TC001529.

Wessel, P. & Smith, W.H.F., 1998. New, improved version of the Generic Mapping Tools released, *EOS Trans. AGU,* **79,** 579.

Wiens, D.A. & Stein, S., 1983. Age dependence of intraplate seismicity and implications for lithospheric evolution, *J. geophys. Res.,* **88,** 6455–6468.